Dominant-negative C/ebpα and polycomb group protein Bmi1 extend short-lived hematopoietic stem/progenitor cell life span and induce lethal dyserythropoiesis

Ting Zhou,[1] Lei Wang,[1] Kang-Yong Zhu,[1] Mei Dong,[1] Peng-Fei Xu,[1] Yi Chen,[1] Sai-Juan Chen,[1] Zhu Chen,[1] Min Deng,[1] and Ting Xi Liu[1-3]

[1]Key Laboratory of Stem Cell Biology and State Key Laboratory of Medical Genomics and Laboratory of Development and Diseases, Institute of Health Sciences, Shanghai Institutes for Biological Sciences, Chinese Academy of Sciences & Shanghai Jiao Tong University School of Medicine, and Shanghai Institute of Hematology, RuiJin Hospital, Shanghai Jiao Tong University School of Medicine, Shanghai, People's Republic of China; [2]Model Organism Division, E-Institutes of Shanghai Universities, Shanghai, People's Republic of China; and [3]Shanghai Stem Cell Institute, Shanghai Jiao Tong University School of Medicine, Shanghai, People's Republic of China

The primitive hematopoietic stem/progenitor cells (HSPCs) during embryonic hematopoiesis are thought to be short-lived (SL) with limited self-renewal potential. The fate and consequence of these short-lived HSPCs, once reprogrammed into "long-lived" in a living animal body, remain unknown. Here we show that targeted expression of a dominant-negative C/ebpα (C/ebpαDN) in the primitive SL-HSPCs during zebrafish embryogenesis extends their life span, allowing them to survive to later developmental stage to colonize the definitive hematopoietic sites, where they undergo a proliferative expansion followed by erythropoietic dysplasia and embryonic lethality because of circulation congestion. Mechanistically, C/ebpαDN binds to a conserved C/EBP-binding motif in the promoter region of *bmi1* gene, associated with a specific induction of *bmi1* transcription in the transgenic embryos expressing C/ebpαDN. Targeted expression of Bmi1 in the SL-HSPCs recapitulates nearly all aberrant phenotypes induced by C/ebpαDN, whereas knockdown of *bmi1* largely rescues these abnormalities. The results indicate that Bmi1 acts immediately downstream of C/ebpαDN to regulate the survival and self-renewal of HSPCs and contribute to the erythropoietic dysplasia. (*Blood*. 2011;118(14):3842-3852)

Introduction

The ontogeny of vertebrate hematopoietic system is a strictly regulated process. The hematopoietic stem cells (HSCs) are able to self-renew and take stepwise differentiation to generate multipotential hematopoietic progenitors and finally produce functional mature cells of all lineages. Another hallmark of HSCs is their mysterious migration and sequential shifts between different organs/locations during early embryonic development.[1,2] Like mammals, the zebrafish hematopoiesis can be divided into 2 successive phases: the primitive and definitive waves. The primitive wave is transient and begins in 2 anatomically and functionally distinct regions: the anterior- and posterior-bilateral plate mesoderm at 12 hours postfertilization (hpf).[3-5] The anterior-bilateral plate mesoderm gives rise to the primitive macrophages and head vasculature,[6-8] and the posterior-bilateral plate mesoderm consists of putative hemangioblasts that migrates medially in an anterior to posterior wave to form the intermediate cell mass (ICM) at 18 hpf. The intraembryonic ICM is thought to be the equivalent of mammalian extraembryonic yolk sac blood island and contains hematopoietic stem/progenitor cells (HSPCs) that are able to generate multipotent blood cell lineages, including a large population of primitive erythrocytes, neutrophilic granulocytes, and platelets. Although expressing hematopoietic transcription factors *scl*, *lmo2*, *gata1*, and *c/ebpα*, these ICM-derived HSPCs are short-lived and possess only short-term or transient hematopoietic activity.[7,9,10] As a result, this primitive hematopoiesis wave gradually wanes after the onset of circulation at 24 hpf. Recently, an anatomic location, termed posterior blood island (PBI) that is the portion of ICM behind the yolk sac extension, has also been shown to initiate bilineage hematopoiesis between 24 and 36 hpf through committed erythromyeloid progenitors (EMPs). The bipotent EMPs also express *scl* and *lmo2* transcripts and possess transient proliferative potential but do not seed the hematopoietic pronephros or thymus.[11] The zebrafish definitive wave is initiated at the ventral wall of dorsal aorta, an evolutionarily conserved anlage of mammalian aorta-gonad-mesonephros (AGM).[12] Distinct from the ICM/PBI-derived short-term HSPCs, the AGM-derived HSPCs possess long-term multipotent hematopoietic activity and self-renewal potential and are able to migrate to the caudal hematopoietic tissue (CHT, equivalent of mammalian fetal liver) through circulation for proliferative expansion, and finally colonize the kidney marrow (equivalent of mammalian bone marrow) and thymus.[13,14] Recently, an elegant study showed a subset of HSPCs expressing *c-myb* and *CD41* migrate anteriorly along the bilateral pronephric ducts (PDs) to colonize the developing pronephros.[15] These PD-HSPCs appeared to originate from the dorsal AGM-HSPCs, whether alternative locations such as PBI or ICM also contribute to the PD-HSPCs is unclear. These observations that the HSPCs' frequent migration to anatomically distinct organs/locations may reflect the fact that the short-term HSPCs have to explore novel hematopoietic microenvironment as more habitable "niche" capable of

Submitted December 28, 2010; accepted June 10, 2011. Prepublished online as *Blood* First Edition paper, August 9, 2011; DOI 10.1182/blood-2010-12-327908.

The online version of this article contains a data supplement.

The publication costs of this article were defrayed in part by page charge payment. Therefore, and solely to indicate this fact, this article is hereby marked "advertisement" in accordance with 18 USC section 1734.

providing extrinsic signals (eg, Wnt, TGF-β, and SHH) to support their survival and self-renewal.

The CCAAT enhancer binding protein-α (C/EBPα) is an essential transcription factor for HSPCs self-renewal and granulopoiesis.[16,17] Heterozygous mutations in *CEBPA* were found in approximately 10% acute myeloid leukemia patients.[18,19] Most of these mutations affect the amino terminus and eliminate expression of the wild-type 42-kDa protein but do not affect a 30-kDa isoform initiated farther downstream. This truncated protein cannot only inhibit the DNA binding of the wild-type C/EBPα in a dominant-negative (DN) manner but seems to have its own functions and potential targets.[20,21] Our previous work showed that the protein and genomic structures of C/EBPα are highly conserved throughout vertebrate evolution. The expression of zebrafish *c/ebpa* is readily detected in the developing HSPCs in the P-LPM/ICM and colocalizes with other hematopoietic stem/progenitor markers, such as *scl*, *lmo2*, *pu.1*, and *gata-1*.[7] A single cytosine deletion mutation (zD420) in zebrafish that mimics the C/EBPα deletion mutation (hD395) found in human with M2-subtype myeloid leukemia shows similar DN activities to its human counterpart hD395 mutant.[7,18] The results suggest that the C/EBPα may play a crucial role in regulating the development and self-renewal of these short-lived HSPCs during embryogenesis, and targeted interference of the C/EBPα signaling through expressing its DN isoform in the developing short-lived HSPCs may provide invaluable insights into the molecular and developmental mechanisms underlying the HSPC self-renewal and diseases.

Although the importance of extrinsic signals in the maintenance of HSPC stemness was clarified, some of the intrinsic factors responsible for HSPC survival and self-renewal have also been identified. Epigenetic regulators, such as the polycomb family proto-oncogene *Bmi1*, have been shown to be important in regulating HSPC proliferation and self-renewal activity. Ablation of Bmi1 function results in the disruption of self-renewal capacity of normal and leukemia stem cells.[22,23] Overexpression of Bmi1 has been found in human high-risk leukemia and other malignancies and is related to unfavorable prognosis.[24,25] Although several targets downstream of Bmi1, including p16Ink4a and p19Arf, have been identified,[23] the upstream signaling pathways regulating *Bmi1* expression remain largely unknown.

Here we show that targeted expression of C/ebpαDN in the ICM/PBI-derived, short-lived, and *scl*-positive HSPCs with limited self-renewal potential extends their life span, allowing them to colonize the bilateral PDs and CHT, where they proliferate and undergo aberrant differentiation along the erythroid lineage, resulting in a massive increase of immature erythrocytes in the circulation and embryonic lethality because of circulation congestion before 14 days postfertilization (dpf). Furthermore, the EGFP-tagged C/ebpαDN directly interacts with an evolutionarily conserved C/EBP binding motif within the promoter region of *bmi1*, concomitant with a specific induction of *bmi1* transcripts in the ICM/PBI-located HSPCs expressing C/ebpαDN. Targeted expression of Bmi1 in the same population of HSPCs recapitulates nearly all C/ebpαDN-induced phenotypes, and knockdown of *bmi1* largely corrects these abnormalities. These studies uncover a mechanistic link between C/ebpα and Bmi1 synergistically to regulate HSPC homeostasis and potential involvement in human erythropoietic disorders.

Methods

Fish care

Zebrafish maintenance, breeding, and staging were performed as previously described.[26] The zebrafish study was approved by the Institute of Health Sciences institutional review board.

Establishment of zebrafish transgenic lines and genomic PCR

Tg (lmo2:Cre) transgenic zebrafish was established in our laboratory as previously described.[27] A 2.5-kb zebrafish *lmo2* promoter fragment[28] was used to direct the expression of LDL-EGFP, LDL-EGFP-C/ebpαDN,[7] and LDL-Bmi1-EGFP. Transgenic plasmids flanked by I-SceI[29] were prepared with an endotoxin-free kit (Promega). Microinjection was performed at one-cell stage embryos with 1- to 1.5-nL of injection solution containing 80 pg/nL of DNA, 0.5× I-SceI buffer and 0.5 U/μL I-SceI meganuclease (New England Biolabs). Injected embryos were raised to sexual maturity (F0 founders) and crossed to wild-type zebrafish to generate F1 progeny, which were screened for the DsRed expression in the ICM/PBI at 22 hpf. The DsRed$^+$ F1 embryos were raised to adults to establish the stable transgenic lines. The adult F1 transgenic zebrafish *Tg(lmo2:LDL-EGFP)*, *Tg(lmo2:LDL-EGFP-C/ebpαDN)*, and *Tg(lmo2:LDL-Bmi1-EGFP)* were crossed to the *Tg* (*lmo2:*Cre) adults to detect the red-green fluorescence shift using a fluorescent stereomicroscope Zeiss SteREO Discovery V20 (Carl Zeiss) with a 1.5× Plan-Apo S objective and AxioVision, Version Rel4.6 software. All the micrographs were taken using 3% methylcellulose as medium. Genomic PCR followed by sequencing was used to validate the Cre recombinase-mediated genomic recombination as previously described.[27] Primer sequences are available in supplemental Table 1 (available on the *Blood* Web site; see the Supplemental Materials link at the top of the online article). The movies of circulation (supplemental Videos 1-3) were taken by a microscope Olympus IX81 with a 20× DIC objective and Image-Pro Plus Version 5.1 software.

Genomic nested PCR

Genomic DNA from the trunk muscle, tail tip, CHT, and the CHT-released blood cells was extracted by Genomic DNA Isolating Kit (BioDev). PCR reactions using specific nested PCR primers indicated in Figure 1C (black and red arrows) were performed as follows: 95°C, 10 minutes; 38 cycles of 94°C, 30 seconds; 55°C, 30 seconds; 68°C, 2.5 minutes; and then 68°C for10 minutes. The PCR products of first round were purified as the templates for a second round reaction: 95°C, 10 minutes; 38 cycles of 94°C, 30 seconds; 55°C, 30 seconds; 68°C, 1.5 minutes; and then 68°C for 10 minutes. Nested PCR products were separated on a 1.5% agarose gel. Primer sequences are available in supplemental Table 1.

Western blot

For Western blot, embryos at indicated developmental stages were deyolked as previously described.[30] Embryos were homogenized in lysis buffer (20mM Tris HCl [pH 7.4], 150mM NaCl, 5mM EDTA, 10% glycerol, and 0.1% Triton X-100). Signals were detected with rabbit anti-EGFP polyclonal antibody (1:1000, Clontech) for overnight at 4°C, followed by incubation with HRP-conjugated secondary antibody (1:10 000).

Cytology assay

Blood cell isolation was performed as described.[31] The 0.9× PBS containing 50 U/mL heparin, 5% FBS, and 0.006% tricaine was used as isolation buffer. For cytospin, the cell collections were centrifuged at 100*g* for 5 minutes onto glass slides. Wright-Giemsa stain was performed according to the manufacturer's instructions (Baso). The micrographs were taken by a microscope Nikon ECLIPSE 80i with 100× oil immersion lens and Nikon ACT-1 software.

Morpholino oligonucleotide knockdown

Zebrafish *bmi1* morpholino oligonucleotides were purchased from Gene Tools and diluted with nuclease-free water. Microinjection of morpholino

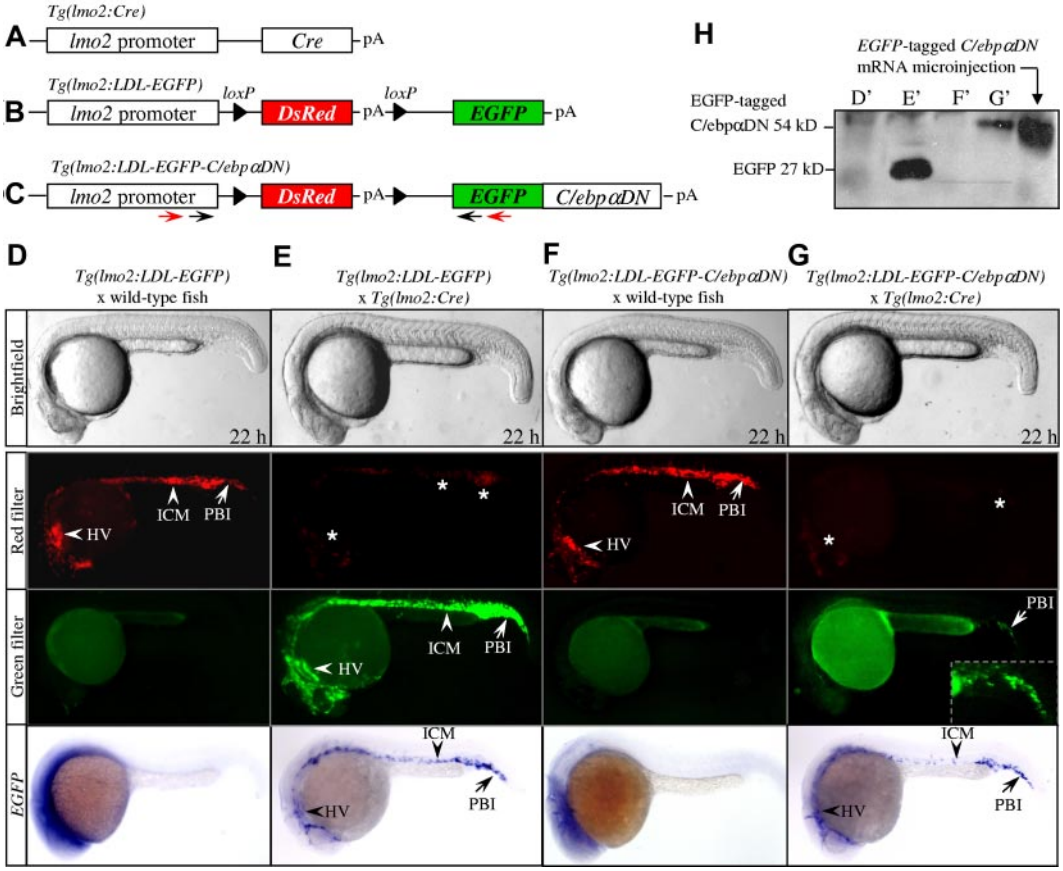

Figure 1. Generation and characterization of stable C/ebpαDN transgenic lines with Cre-loxp strategy. (A-C) Schematic representations of transgenic lines *Tg(lmo2:Cre)* (A), *Tg(lmo2:LDL-EGFP)* (B), and *Tg(lmo2:LDL-EGFP-C/ebpαDN)* (C). All transgenes were under the control of a 2.5-kb *lmo2* promoter. The *EGFP* or *EGFP*-tagged *C/ebpαDN* gene was separated from the *lmo2* promoter by *loxp*-DsRed-*loxp* (*LDL*) element. Truncated zebrafish *C/ebpαDN* was in-frame fused with *EGFP*. Arrows at the bottom of panel C indicate the position of primers used in genomic PCR for genotyping. pA indicates SV40 polyadenylation site. (D-G) Representative 22 hpf progeny of mating *Tg(lmo2:LDL-EGFP)* with either wild-type (D) or *Tg(lmo2: Cre)* heterozygote (E), and mating *Tg(lmo2:LDL-EGFP-C/ebpαDN)* with either wild-type (F) or *Tg(lmo2:Cre)* heterozygote (G). Red-green fluorescence shifts can only be detected in the double-transgenic embryos carrying the *Cre* recombinase gene (E,G). The stars indicate the residual red fluorescence after Cre-mediated genomic recombination. HV indicates head vasculature. (H) Western blot analyses confirmed the expression of EGFP (27 kDa) and EGFP-tagged C/ebpαDN fusion protein (54 kDa) in the transgenic embryos presented in panels D to G corresponding to lines D′ to G′.

oligonucleotides was performed at one- or two-cell stage. All injections were performed with Harvard Apparatus microinjector. Morpholino sequences are available in supplemental Table 1.

WISH

Whole-mount mRNA in situ hybridization (WISH) was performed as described previously.[32] For embryos older than 48 hpf, high resolution of WISH was performed as previously described.[13] For 2-color in situ hybridization, the *scl* antisense RNA probe was labeled with digoxigenin (Roche Diagnostics), whereas antisense probes against *EGFP* were labeled with fluorescein (Roche Diagnostics). The purple color was developed first with nitroblue tetrazolium/5-bromo-4-chloro-3-indolyl-phosphate (Vector Laboratories) as a substrate, followed by the development of red color with Fast Red tablets (Roche Diagnostics). The results were imaged using a stereomicroscope Nikon SMZ1500 with 1× HR Plan Apo objective and ACT-1 vision software. Embryos were mounted in 95% glycerol.

Immunochemistry and TUNEL assays

Whole-mount immunochemistry staining for proliferation was performed with a rabbit polyclonal antibody against phosphorylated histone 3 (pH3) as previously described.[33] Whole-mount TUNEL assay was performed using POD in situ Cell Death Detection Kit (Roche Diagnostics) according to the manufacturer's instructions. All results were imaged by stereomicroscope Nikon SMZ 1500 with 1× HR plan Apo objective and Version ACT-1 software.

E-ChIP

Embryos at 22 hpf were enzymatically dechorionated and then fixed in 1.85% formaldehyde. Embryonic chromatin immunoprecipitation (E-ChIP) with a polyclonal antibody against EGFP (Clontech) was performed as previously described.[34] The 15 and 10 kb of potential promoter sequences upstream of the transcriptional start site (TSS) of murine and zebrafish *bmi1* gene, respectively, were analyzed with rVista software (http://genome.lbl.gov/vista/rvista/submit.shtml). Potential C/EBP binding motifs were identified (http://www.genome.jp/tools/motif). Primer sequences are available in supplemental Table 1.

Results

Establishment and characterization of C/ebpαDN transgenic zebrafish lines

The zebrafish *C/ebp*αDN (previously designated as zD420 and termed C/ebpαDN hereafter) carries a deletion at the evolutionarily conserved cytosine, which is also found in human patient with M2-subtype acute myeloid leukemia (previously designated as hD395).[7,18] The C/ebpαDN deletion mutation prevents expression of the full-length protein, allowing the expression of truncated isoforms from internal translational initiation sites, and has similar DN activities as its human counterpart hD395.[7] To investigate the

function of C/ebpαDN in the developing HSPCs, we took use of a previously established *Tg(lmo2:Cre)* transgenic line (Figure 1A)[27] and first established 2 novel transgenic lines, *Tg(lmo2:LDL-EGFP)* (Figure 1B) and *Tg(lmo2:LDL-EGFP-C/ebpαDN)* (Figure 1C), in which a floxed *DsRed* gene (*loxP-DsRed-loxP*, abbreviated as *LDL*) followed by either a downstream *EGFP* or an in-frame fused *EGFP-C/ebpαDN* gene, are expressed under the *lmo2* promoter,[28] respectively. Because the *lmo2* transcripts are richly detected in the developing HSPCs and bipotential EMPs in the ICM and PBI regions,[2,11] the combinational use of the *Tg(lmo2:Cre)* and the *Tg(lmo2:LDL-EGFP-C/ebpαDN)* transgenic lines provides an invaluable tool to investigate the function of the leukemogenic C/ebpαDN in the short-lived HSPCs in a physiologic context.

The control *Tg(lmo2:LDL-EGFP)* and the *Tg(lmo2:LDL-EGFP-C/ebpαDN)* heterozygous transgenic adults were first mated to either wild-type or *Tg(lmo2:Cre)* heterozygote to evaluate the Cre recombinase activity in vivo through examining the shift of red fluorescence to green fluorescence at 22 hpf. In the *LDL-EGFP*$^{+/-}$;*wild-type* embryos, only red fluorescence was detected in the head vasculature, ICM, and PBI (Figure 1D; red filter), without any detectable EGFP fluorescence (Figure 1D; green filter). In the double-transgenic *LDL-EGFP*$^{+/-}$;*Cre*$^{+/-}$ embryos, however, only residual red fluorescence was retained (Figure 1E stars; red filter), with robust EGFP fluorescence being observed in the head vasculature, ICM, and PBI (Figure 1E; green filter). Highly similar fluorescent expression and shift patterns were also observed in the *LDL-EGFP-C/ebpαDN*$^{+/-}$;*wild-type* and *LDL-EGFP-C/EBPαDN*$^{+/-}$;*Cre*$^{+/-}$ embryos (Figure 1F-G), except that the EGFP fluorescence of *LDL-EGFP-C/ebpαDN*$^{+/-}$;*Cre*$^{+/-}$ embryos was weaker than that of *LDL-EGFP*$^{+/-}$;*Cre*$^{+/-}$ embryos (Figures 1E,G; green filters). The EGFP fluorescence was predominantly detected in the PBI of the *LDL-EGFP-C/ebpαDN*$^{+/-}$;*Cre*$^{+/-}$ embryos (Figure 1G arrowhead; green filter), a site that hosts the short-lived bipotent hematopoietic progenitor (EMP) development and forms the CHT (equivalent of mammalian fetal liver) at later stages (48 hpf to 7 dpf).[11,13,35] WISH analyses using a digoxigenin-labeled *EGFP* antisense probe verified these results (Figure 1D,G bottom panels). In addition, Western blot analyses confirmed the expression of the EGFP (27 kDa) and the EGFP-tagged C/ebpαDN proteins (54 kDa) in the lysates of *LDL-EGFP*$^{+/-}$;*Cre*$^{+/-}$ and *LDL-EGFP-C/ebpαDN*$^{+/-}$;*Cre*$^{+/-}$ embryos at 22 hpf, respectively (Figure 1H lanes E′ and G′). Furthermore, genomic PCR (primer locations indicated by black arrows in Figure 1C) and subsequent sequencing analyses confirmed that the Cre-mediated recombination occurred precisely at the LoxP sites (supplemental Figure 1; and data not shown).

Circulation congestion and erythropoietic dysplasia in the transgenic embryos expressing C/ebpαDN

Because the *lmo2* promoter is activated during primitive hematopoiesis (12-26 hpf) and gradually wanes as definitive hematopoiesis initiates in the AGM at 26 hpf and expands in the CHT from 48 hpf onwards,[2,28] the EGFP fluorescence in the *EGFP-C/ebpαDN* transgenic embryos was hardly detected after 24 hpf. Consistently, Western blot analyses showed that the expression of EGFP-tagged C/ebpαDN protein was undetected at 36 and 75 hpf but still weakly expressed at 26 hpf (supplemental Figure 2). We therefore picked out the EGFP-positive embryos at 22 hpf from the clutches of mating the *Tg(lmo2:Cre)* heterozygote to either *Tg(lmo2:LDL-EGFP)* or *Tg(lmo2:LDL-EGFP-C/ebpαDN)* heterozygote. These EGFP-positive embryos carrying either *LDL-EGFP*$^{+/-}$;*Cre*$^{+/-}$ or *LDL-EGFP-C/ebpαDN*$^{+/-}$;*Cre*$^{+/-}$ double transgenes were subject to intensive visual investigation, and no any detectable morphologic abnormalities were found before 72 hpf. Starting at 75 hpf, however, 98% of *EGFP-C/ebpαDN*-positive embryos (n = 65/66) demonstrated a congested circulation with blood cells accumulated within the caudal vein of CHT, which resulted in a deteriorating cardiac edema and embryonic lethality between 7 and 14 dpf (Figure 2A-B arrows; supplemental Videos 1 and 2; and data not shown). No obvious abnormalities were observed in the heart and vasculature development (data not shown). To confirm whether the accumulated blood cells had undergone Cre-mediated genomic recombination, we performed nested genomic PCR with 2 specific primer pairs (Figure 1C black and red arrows) to genotype the DNA extracted from the dissected tissue or the released blood cells in indicated anatomic sites (Figure 2B: I, tail tip; II, CHT; III, trunk muscle indicated by red boxes; and IV, CHT released blood cells indicated by curved arrow). As shown in Figure 2B and C, a 0.3-kb recombinant fragment was exclusively amplified from the CHT-released blood cells (IV), whereas only a 1.5-kb unrecombinant fragment was obtained from the tail tip (I). As expected, the CHT and trunk-derived muscle showed a stronger unrecombinant fragment and a weaker recombinant fragment probably because of the contamination of blood cells within these tissues (II and III). The Giemsa staining of the released cells from the congested CHT showed immature erythroid morphology with higher nucleus-cytoplasm ratio, basophilic staining, and cells undergoing mitotic division (Figure 2D-E arrow). Furthermore, a significantly increased number of cells positive for the mitotic pH3 marker (Figure 2F-G arrow) and the apoptotic TUNEL staining (Figure 2H-I arrows) was also observed in the congested CHT and segmental vessels of *EGFP-C/ebpαDN*-positive embryos.

To characterize the molecular nature of these dysplastic blood cells, we performed WISH analyses with hematopoietic marker genes (α-*E1* and α-*E3* hemoglobin for embryonic erythroid cells; *gata-1* for erythroid progenitors; *mpo* and *l-plastin* for embryonic neutrophilic granulocytes and monocytes/macrophages, respectively; and *rag-1* for thymic lymphocytes) at various developmental stages from 22 to 75 hpf. Although no obvious changes for the erythroid α-*E1* and α-*E3* expression were detected at 22 and 26 hpf (supplemental Figure 3A), a significantly increased number of α-*E1*– and α-*E3*–expressing erythroid cells was observed at 75 hpf: in the *EGFP*-positive control embryos at 75 hpf, α-*E1*- and α-*E3*–positive erythroid cells were mainly detected in the regions of heart and CHT (Figure 3A; supplemental Figure 3B, star and arrow); in the *EGFP-C/ebpαDN*-positive embryos, however, the *globin*-expressing cells abundantly filled in the cardiac region (star), the trunk vessels (red arrow), dorsal aorta (red arrowheads), cranial vasculature (red arrowheads), and segmental vessel (black arrowheads) (Figure 3B; supplemental Figure 3C). No changes in the levels of *gata-1* transcripts were detected at 22, 36, and 75 hpf (supplemental Figure 4), suggesting that a Gata-1–independent mechanism contributed to the erythropoietic dysplasia. A slight increase, if any, was also observed for the expression of *l-plastin* and *mpo* at 75 hpf (supplemental Figure 5; and data not shown). In addition, a robust reduction or lack of *rag-1* expression was also detected in the developing thymus, probably resulting from the disrupted circulation that is required for HSCs to colonize the thymus (supplemental Figure 6).[13] Thus, the congested circulation observed in the CHT of *EGFP-C/ebpαDN*-positive embryos at 75 hpf resulted from a dysplasia of immature erythrocytes that had undergone Cre-mediated genomic recombination and were progeny of the C/ebpαDN-expressing HSPCs derived from ICM/PBI at 22 hpf.

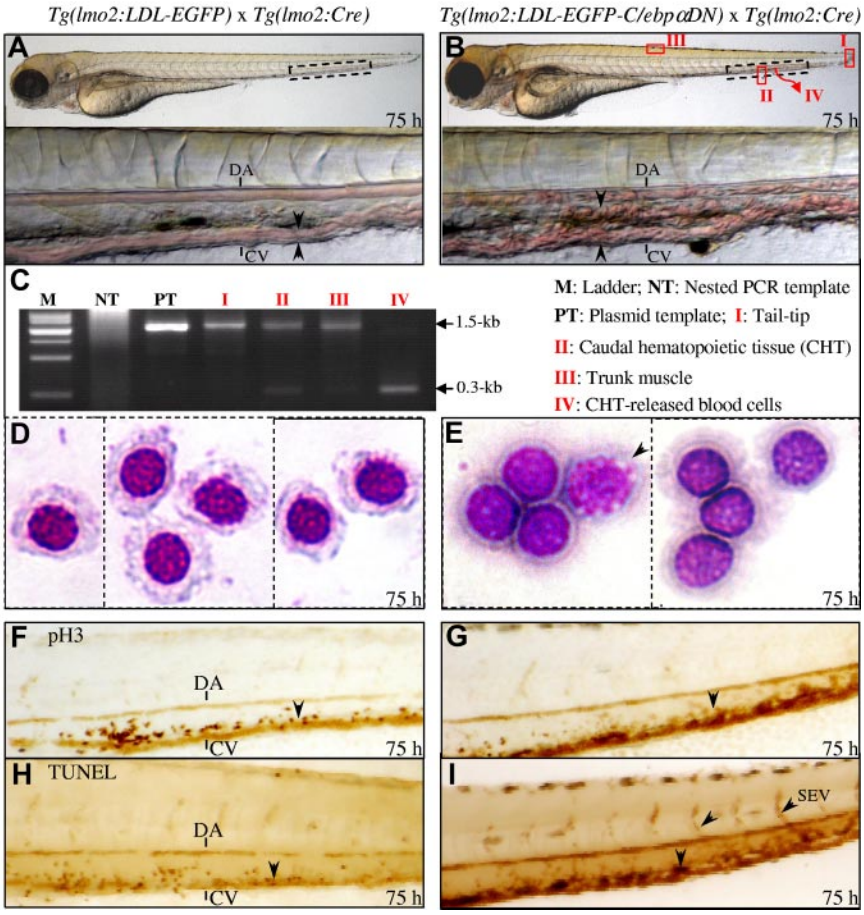

Figure 2. Circulation congestion and erythropoietic dysplasia in the C/ebpαDN transgenic embryos. (A-B) External features of the *Tg(lmo2:LDL-EGFP)* (A) and *Tg(lmo2:LDL-EGFP-C/ebpαDN)* (B) embryos at 75 hpf. The circulation congestion is only detected in the C/ebpαDN-expressing embryos (B, arrowheads and supplemental Videos 1 and 2). Black boxes with dashed lines indicate the regions amplified at the bottom. Red boxes and curved arrow indicate the sites where tissue or circulating cells were isolated and genomic DNA were extracted for genotyping shown in panel C. DA indicates dorsal aorta; and CV, caudal vein. (C) Analyses of Cre-mediated genomic recombination by genomic-nested PCR using 2 pairs of primers indicated at the bottom of Figure 1C. The Roman numerals indicate the anatomic sites where tissues and cells are dissected (I-III) or released from the CHT (IV). (D-E) Wright-Giemsa stainings and morphologic characterizations of circulating blood cells released from the CHT of transgenic embryos at 75 hpf from *Tg(lmo2:LDL-EGFP)*. (D) All 3 panels are adopted from the same slide and composited together and *Tg(lmo2:LDL-EGFP-C/ebpαDN)*. (E) Both panels are adopted from the same slide. Arrow indicates the cell undergoing mitosis. Images were acquired with a 100× oil objective. (F-I) Proliferation and apoptosis analyses by pH3 immunochemistry stainings (F-G) and TUNEL assays (H-I) in the embryos expressing EGFP and EGFP-C/ebpαDN at 75 hpf as described in "Immunochemistry and TUNEL assays."

Developmental origin and mechanism of erythropoietic dysplasia induced by C/ebpαDN

The PBI/ICM-derived HSPCs (including EMPs in the PBI region) occurred in the primitive hematopoiesis wave are thought to be transient and short-lived with limited self-renewal ability. As a result, they become hardly detected by WISH using *scl* or *lmo2* as a marker after 24 hpf and do not contribute to the definitive hematopoiesis initiating in the AGM (between 26 and 72 hpf) and subsequently expanding in the CHT (between 48 hpf and 7 dpf).[11] How could these short-lived PBI/ICM-derived primitive HSPCs contribute to the dyserythropoiesis occurrence at the definitive hematopoiesis stage at 75 hpf? One possible explanation is that the C/ebpαDN extends the life span and promotes the self-renewal of these short-lived HSPCs, therefore allowing them to colonize the definitive hematopoiesis sites, such as CHT for proliferative expansion and aberrant erythroid differentiation. Because these PBI/ICM-derived HSPCs express the stem cell maker gene *scl*,[36] we first performed time-course WISH analyses with *scl* as a probe to trace the developmental origin of the erythropoietic dysplasia. Consistent with the hypothesis, a significantly increased number of *scl*$^+$ HSPCs was readily detected in the CHT region of C/ebpαDN-positive embryos (n = 14 of 19) at 75 hpf, compared with the *EGFP*$^+$ control embryos (Figure 3C-D). Unexpectedly, a 4-fold increase (3.3 vs 11.6) of the *scl*$^+$ HSPCs was also detected in the bilateral PDs at 36 hpf (Figure 3E-F arrows) and 30 hpf (Figure 3G-H arrows), although no such change was detected at 22 hpf (Figure 3I-J). This finding is intriguing in that the PD was recently shown to serve as a migratory path for the HSPCs (*c-myb*$^+$*CD41*$^+$) to colonize the developing glomerulus.[15]

As expected, these *scl*$^+$ PD-HSPCs also expressed *EGFP-C/ebpαDN* transcripts as determined by double WISH (Figure 3K-L, arrows), suggesting that these PD-HSPCs are progeny of PBI/ICM-derived HSPCs that expressed C/ebpαDN. Collectively, the results suggested a model that targeted expression of C/ebpαDN in these *scl*$^+$ PBI/ICM-HSPCs at 22 hpf and resulted in an extended life span, allowing them to colonize the PD and the CHT, where they underwent proliferative expansion and Gata-1-independent dyserythropoiesis at 75 hpf.

Specific up-regulation of *bmi1* transcripts in the PBI/ICM-located HSPCs

To explore the possible molecular mechanisms responsible for the C/ebpαDN-induced extension of HSPCs' life span, we screened a panel of zebrafish orthologs of mammalian epigenetic and developmental regulators that have been shown essential for self-renewal of HSCs and leukemia stem cells. These genes are *bmi1*,[22] *prdm3*,[37] *prdm16*,[38] *ezh2*, *rae28*, *notch1a*, *her6*, *cdx4*, *cdx1a*, *hox9a*, *hoxb4*,[39] and *sonic hedgehog* (*shh*).[40] Interestingly, of 12 self-renewal genes screened, 4 genes (*bmi1*, *rae28*, *prdm3*, and *prdm16*) are specifically induced in the PBI and/or ICM regions (Figure 4 arrows) and no changes were detected for the other 8 genes (*shh*, *notch1a*, *her6*, *ezh2*, *cdx4*, *cdx1a*, *hoxa9*, and *hoxb4*; supplemental Figure 7). Of 4 induced genes, the significant induction of *bmi1* transcripts specifically in the PBI and ICM (Figure 4A-B arrows) is particularly interesting because the Cre recombinase activity and EGFP-C/ebpαDN expression were also detected in these 2 regions (Figure 1G), suggesting that the Bmi1 may act downstream of C/ebpαDN signaling to mediate the expansion of the *scl*$^+$ HSPCs

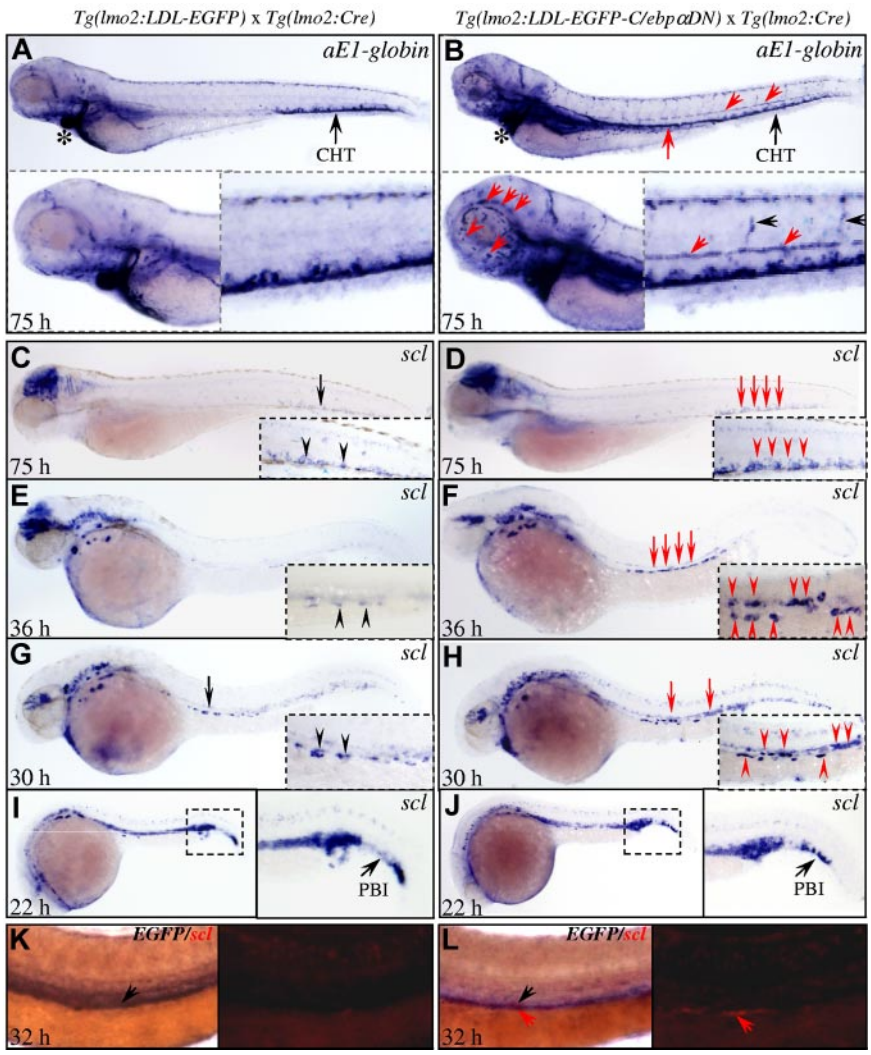

Figure 3. Developmental mechanism and origin of dyserythropoiesis. (A-B) WISH analyses of α*E1-globin* in the indicated transgenic embryos at 75 hpf. The star, red arrow, and arrowheads indicate the increased number of erythrocytes expressing α*E1-globin* transcripts within the embryonic vasculature. (C-J) Time course of WISH analyses of *scl* in the transgenic embryos at indicated developmental stages. Red arrows and arrowheads indicate the increased *scl*$^{+}$ HSPCs in the CHT and bilateral PDs. (K) Two-color WISH of *EGFP* (black color) and *scl* (red color) transcripts in the transgenic embryos at 32 hpf. (K-L) Fast red labeling of *scl* (RITC filter) is shown to the right. The red and black arrows indicate the colocalization of *scl* and *EGFP*.

and extension of their life span in the bilateral PD (30-36 hpf) and CHT (75 hpf), which in turn caused erythropoietic dysplasia.

Targeted overexpression of Bmi1 in the PBI/ICM-located HSPCs recapitulates phenotypes induced by C/ebpαDN

To test the hypothesis, we established another stable transgenic line *Tg(lmo2:LDL-Bmi1-EGFP)* to specifically express the EGFP-tagged Bmi1 protein in the HSPCs of PBI/ICM (Figure 5A). The zebrafish Bmi1 protein located on chromosome 24 shares 80% and 81% amino acid identities with its human and murine counterparts, respectively (data not shown). By mating the *Tg(lmo2:LDL-Bmi1-EGFP)* heterozygote to the *Tg(lmo2:Cre)* heterozygote, targeted expression of Bmi1-EGFP in the HSPCs of PBI/ICM was verified in both EGFP fluorescence and transcript levels at 22 hpf (Figure 5B, arrow and arrowhead). Time-course WISH analyses showed that the number of *scl*$^{+}$ HSPCs was unchanged at 22 hpf (Figure 5C-D) but significantly increased along the bilateral PD in the *LDL-Bmi1-EGFP*$^{+/-}$;*Cre*$^{+/-}$ embryos at 36 hpf (Figure 5E-H arrows and arrowheads in the inset). More importantly, the morphologic phenotypes characterized by circulation congestion (Figure 6A-B) and accumulation of hematopoietic cells positive for both pH3 (Figure 6C-D) and TUNEL staining (Figure 6E-F) in the CHT region, along with a massive increase of the α-*E1*-positive erythroid cells throughout the embryos (Figure 6G-H), were also observed in the *LDL-Bmi1-EGFP*$^{+/-}$;*Cre*$^{+/-}$ embryos at 80 hpf. The results indicate that targeted expression of Bmi1 protein in the PBI/ICM-located HSPCs recapitulates most, if not all, of the morphologic and molecular abnormalities observed in the C/ebpαDN transgenic embryos and suggest that the self-renewal enhancement and life span elongation of the short-lived, *scl*$^{+}$ HSPCs are conferred by transcriptional activation of *bmi1* by C/ebpαDN.

Bmi1 is a direct downstream target of C/ebpαDN

The specific induction of *bmi1* in the *Tg(lmo2:LDL-EGFP-C/ebpαDN)* embryos and highly similar phenotypes between the *Tg(lmo2:LDL-EGFP-C/ebpαDN)* and *Tg(lmo2:LDL-Bmi1-EGFP)* transgenic lines suggest that the Bmi1 may act downstream of C/ebpαDN. Indeed, injection of a zebrafish *bmi1*-specific morpholino oligonucleotide (supplemental Figure 8) efficiently relieved the C/ebpαDN-mediated circulation congestion and erythropoietic dysplasia (Figure 7A-G). Of 50 C/ebpαDN-positive embryos microinjected with *bmi1*-specific morpholino oligonucleotides (0.15mM), 80% showed no detectable circulation congestion and α-*E1* abnormalities (Figure 7C,F-G). In contrast, in the C/ebpαDN-positive embryos microinjected with an unrelated mismatch morpholino oligonucleotide (0.15mM), 98.5% (65 of 66) maintained these abnormal phenotypes induced by C/ebpαDN (Figure 7B,E,G).

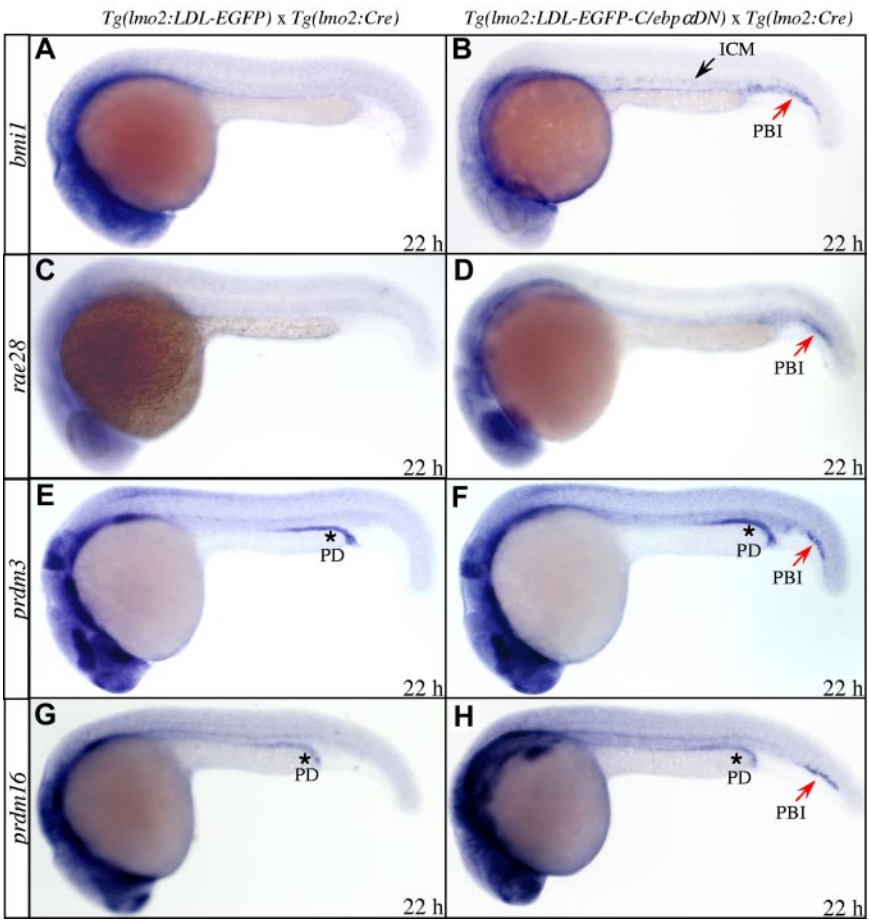

Figure 4. Specific induction of epigenetic regulatory genes by C/ebpαDN. (A-H) WISH analyses of a panel of epigenetic regulators involved in the HSC maintenance and self-renewal at 22 hpf. The arrows indicate the specific induction of *bmi1* (A-B), *rae28* (C-D), *prdm3* (E-F), and *prdm16* (G-H) transcripts in the ICM or PBI region.

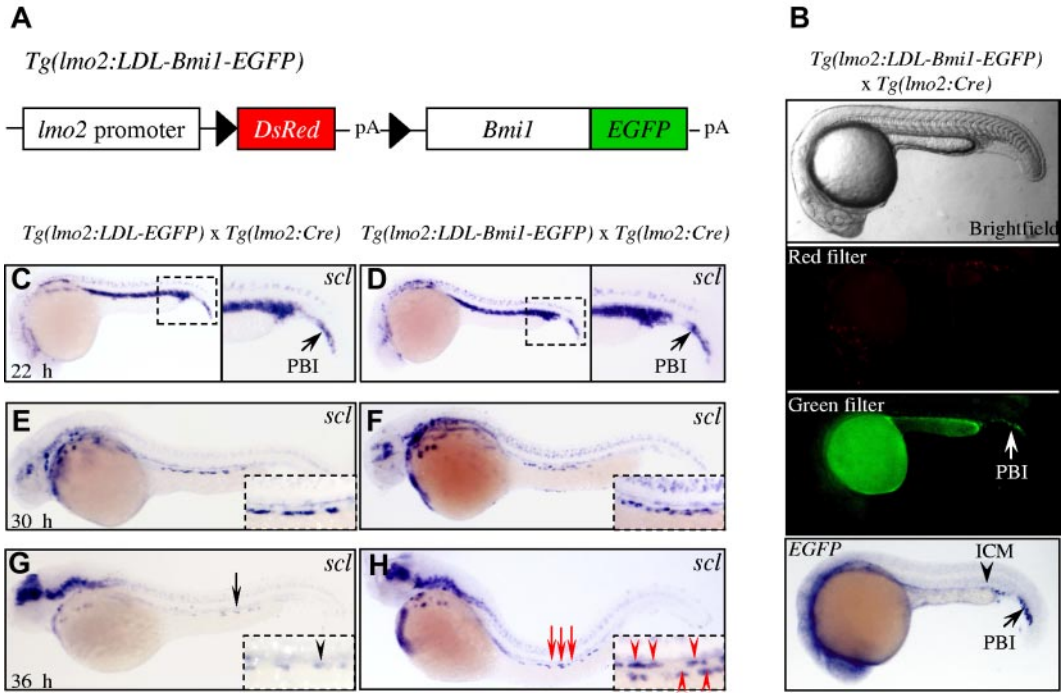

Figure 5. Characterization of Bmi1 transgenic zebrafish line. (A) Schematic representation of *lmo2*:LDL-Bmi1-EGFP transgenic construct. pA indicates SV40 polyadenylation site. (B) Expression of Bmi1-EGFP fusion protein and transcripts in the progeny of mating *Tg(lmo2:LDL-Bmi1-EGFP)* with *Tg (lmo2:Cre)* line. (C-H) time-course WISH analyses of *scl* in the Bmi1-expressing transgenic embryos at indicated developmental stages. Red arrows and arrowheads indicate the increased *scl*$^{+}$ HSPCs along the PD at 36 hpf.

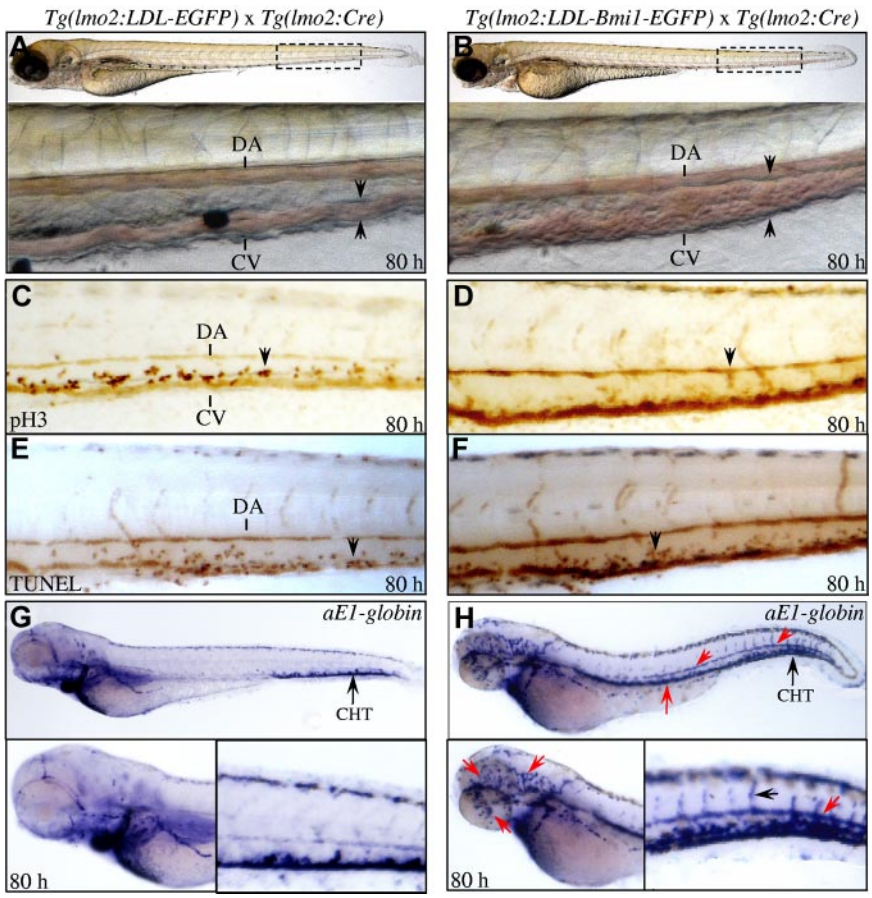

Figure 6. Capitulation of C/ebpαDN-induced abnormalities in the Bmi1 transgenic embryos. (A-B) External features of the *Tg(lmo2:LDL-EGFP)* (A) and *Tg(lmo2:LDL-Bmi1-EGFP)* (B) embryos at 80 hpf. The circulation congestion is readily detected in the Bmi1-expressing embryos (B, arrowheads; and supplemental Videos 1 and 3). Black boxes with dashed lines indicate the regions amplified at the bottom. DA indicates dorsal aorta; and CV, caudal vein. (C-F) Proliferation and apoptosis analyses by pH3 immunochemistry stainings (C-D) and TUNEL assays (E-F) in the embryos expressing EGFP and Bmi1-EGFP at 80 hpf. (G-H) WISH analyses of *αE1-globin* in the transgenic embryos at 80 hpf. The star, red arrow, and arrowheads indicate the increased number of cells with expression of *αE1-globin* transcripts within the embryonic vasculatures.

Moreover, WISH analyses showed that not only the number of the *scl*$^{+}$ HSPCs in the PD region of C/ebpαDN embryos at 36 hpf was reduced to normal level (supplemental Figure 9), but the enhanced proliferation (supplemental Figure 10) and enhanced apoptosis (supplemental Figure 11) were also reversed by *bmi1* knockdown. As a control, injection of either *bmi1*-specific or control morpholino into EGFP control embryos did not cause detectable morphologic and hematopoietic abnormalities (supplemental Figure 12). To further validate whether Bmi1 is a direct downstream target, we analyzed the 20-kb promoter region upstream of the TSS of zebrafish and murine *bmi1* genes and found one evolutionarily conserved region containing a C/EBP binding motif at 5.2 kb upstream of the zebrafish *bmi1* TSS (Figure 7H). The region shares 63% nucleotide acid identities with a region (−11 780 to −11 612 bp) located at the upstream of the murine *Bmi1* TSS (Figure 7I, red dots). We therefore tested whether the EGFP-tagged C/ebpαDN was able to directly bind to this C/EBP motif as well as additional predicted C/EBP motifs indicated by the diamonds in Figure 7H (bottom) by whole E-ChIP assays. Chromatin fragments were extracted from the EGFP$^{+/-}$;Cre$^{+/-}$ and EGFP-C/ebpαDN$^{+/-}$;Cre$^{+/-}$ transgenic embryos at 22 hpf, when the specific up-regulation of *bmi1* transcripts has been readily detected (Figure 4A-B), and were immunoprecipitated with a polyclonal anti-EGFP antibody. DNA from the immunoprecipitates was amplified by PCR using primers located to the indicated genomic regions (I-XI, Figure 7H horizontal lines). The results showed that EGFP-tagged C/ebpαDN specifically interacted with the distant C/EBP motif II (Figure 7J-K). A slightly increased binding activity was also detected for the C/EBP motif I (Figure 7J-K). No binding activity was detected for other regions (Figure 7J-K). The results indicated that Bmi1 is a direct downstream target of C/ebpαDN signaling to promote the self-renewal of these short-lived, *scl*$^{+}$ and PBI/ICM-derived HSPCs, allowing them to colonize the bilateral PD and CHT, where they initiate an abnormal proliferation and differentiation program toward erythroid lineage.

Discussion

In this study, we show, for the first time, a novel genetic and mechanistic link between the leukemogenic mutation C/ebpαDN and stem cell self-renewal regulator Bmi1, and how the C/ebpαDN-Bmi1 signaling axis acts as an intrinsic factor to extend the life span of the short-lived HSPCs with limited self-renewal potential during primitive hematopoietic wave. Once these transient HSPCs are reprogrammed into "long-lived," they are able to survive into definitive hematopoiesis stage and colonize the definitive hematopoietic sites, where they undergo proliferative expansion resulting in severe dyserythropoiesis and embryonic lethality because of circulation congestion and cardiac edema.

Although the human and zebrafish C/ebpαDN were shown to inhibit the function of wild-type full-length C/ebpα in a DN fashion, the possibility of C/ebpαDN gain of function has not been formally excluded. Recently, we and others showed that the C/EBPαDN is able to bind to the promoters of α-*catenin*,[21] *MMP11*, *p84N5*, and *SMYD2*[20] to suppress their transcription through recruiting transcription repressive complex PRC2 and subsequent trimethylation of H3K27,[21] suggesting that C/EBPαDN acquires a novel function other than its ability to inactivate wild-type C/EBPα. Intriguingly, the current study also indicates

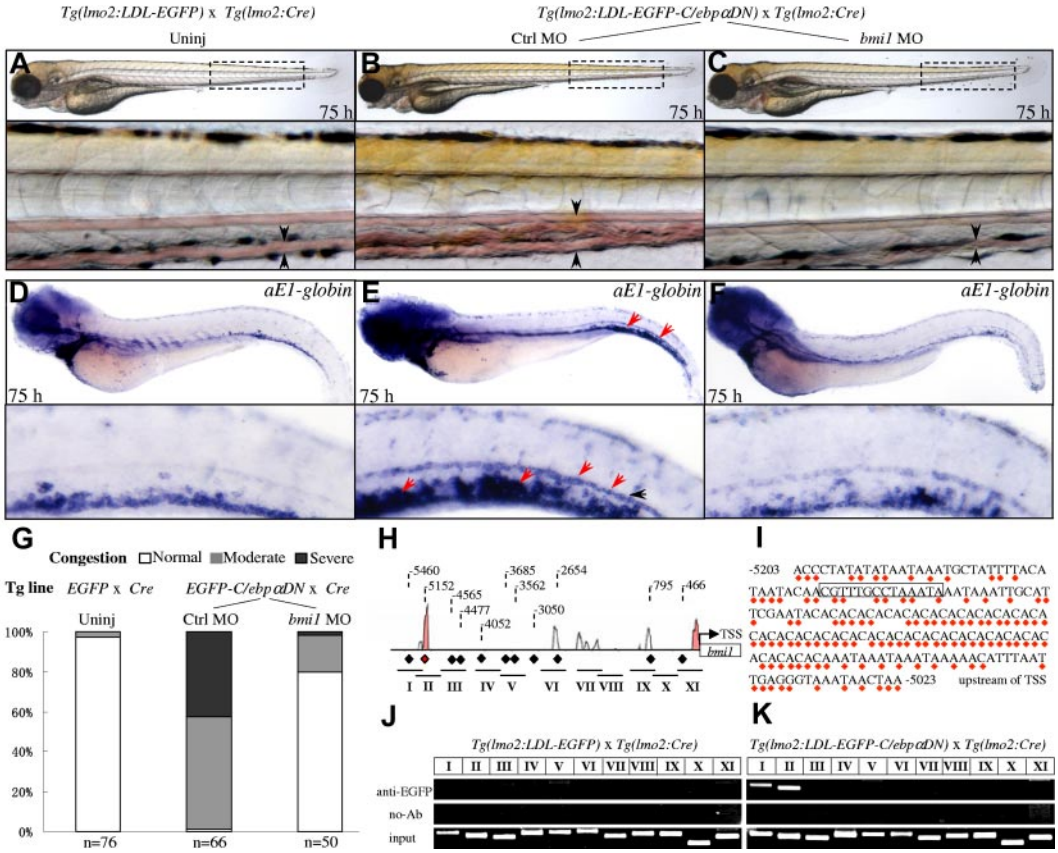

Figure 7. Bmi1 is a direct downstream target of C/ebpαDN. (A-C) External features of the *LDL-EGFP*$^{+/-}$;Cre$^{+/-}$ transgenic embryos without injection (A, uninj), and the *LDL- EGFP-C/ebpα*$^{+/-}$;Cre$^{+/-}$ transgenic embryos injected with either unrelated 5-mismatch (B) or *bmi1*-specifcic morpholino oligonucleotides (C). The circulation congestion is readily detected in the C/ebpαDN-expressing embryos injected with control morpholino (B, arrowheads) but largely rescued by *bmi*1 knockdown (C, arrowheads). Boxes with dashed lines indicate the regions amplified and shown at the bottom. (D-F) WISH analyses of *αE1-globin* in the indicated transgenic embryos at 80 hpf. The red arrowheads indicate that the increased number of erythrocytes with expression of *αE1-globin* transcripts can be corrected to normal level in the *LDL-EGFP-C/ebpα*$^{+/-}$;Cre$^{+/-}$ embryos injected with the *bmi1*-specifcic morpholino oligonucleotide (F). (G) Statistics of circulation congestion in the transgenic embryos shown in panels A to C. Normal, Moderate, and Severe indicate the extent of circulation congestion at the CHT region. (H) Conservation of the zebrafish *bmi1* promoter region 5.5 kb upstream of the TSS with murine *Bmi1* promoter region by rVista software. Diamonds and corresponding dashed lines with Arabic numerals represent the positions of 11 predicted C/EBP binding motifs. Horizontal lines with Roman numerals I to XI indicate the locations of primers used in the E-ChIP analyses. (I) The nucleotide acid sequence of the zebrafish *bmi1* promoter region between −5203 and −5023 bp, corresponding to the conserved region indicated by the red diamond in panel H. Red dots indicate the nucleotide acid identities compared with murine *bmi1* promoter region between −11 780 and −11 612 bp upstream of TSS. The predicated C/EBP binding motif is indicated by a box. (J-K) E-ChIP analyses of chromatins extracted from the *LDL-EGFP*$^{+/-}$;Cre$^{+/-}$ and *LDL-EGFP-C/ebpα*$^{+/-}$;Cre$^{+/-}$ embryos at 22 hpf. PCR reactions were performed using the primers located to the indicated promoter region (I-XI) in panel H. The EGFP-tagged C/ebpα specifically interacts with the C/EBP binding motifs II and I. The results were repeated 3 times with separate clutches of embryos and batches of chromatin preparations.

that the C/ebpαDN can also act as a transactivator to directly or indirectly induce the expression of a panel of important epigenetic regulatory genes, including *bmi1* and *rae28* and set domain-containing genes *prdm3* and *prdm16*, all of which have been reported to be critical for HSC self-renewal and/or leukemia transformation.[32,37,41-43] In addition, our results did not exclude the possibility that the C/ebpαDN interacts with wild-type C/ebpα as a heterodimer at the promoter region of *bmi1* gene to reverse the transcription suppressive effect endowed by full-length C/ebpα. In support of this model, the wild-type *c/ebpα* transcripts are detected in both HSPC-containing ICM and EMP-containing PBI regions (supplemental Figure 13). In addition, an increased level of *Bmi1* has been observed in C/ebpα-deficient murine HSCs.[16] To clarify the issue, a zebrafish C/ebpα antibody needs to be generated to test whether the wild-type C/ebpα also binds to the *bmi1* promoter in a physiologic context. In any case, the current studies suggest that the C/ebpαDN is an important upstream signaling of epigenetic regulators to maintain HSC life span and probable stemness or self-renewal.

In addition to the demonstration of the C/ebpαDN-Bmi1 signaling as a regulator of HSPC activity, the study also uncovers a novel genetic evidence for the involvement of C/ebpαDN-Bmi1 in erythroid proliferative disorders. Although increased numbers of erythroid progenitors and erythroid cells in C/EBPα$^{-/-}$ fetal liver have been documented,[44] and the C/ebpα deficiency fails to induce a bcr/abl-mediated murine myeloid leukemia but contributes to a fatal erythroleukemia instead,[45] the underlying mechanism has not been defined. The *Bmi1* is originally cloned from a human erythroleukemia cell line K562,[46] and its role in erythropoiesis remains to be elucidated. It is probable that the increased erythropoiesis by Bmi1 is only a consequence of both short-lived HSPC expansion and differentiation in a microenvironment or "niche " in the CHT region favoring erythroid fate. However, the possibility of direct involvement of Bmi1 in erythroid commitment and differentiation through epigenetic regulation of other erythroid-specific signaling transduction pathways rather than Gata-1–associated signaling needs to be excluded. In any case, the possible involvement of C/EBPαDN-Bmi1 axis in human erythroid disorders associated with dysplasia, such as polycythemia and erythroleukemia, warrants further investigation.

The bilateral PD was recently demonstrated to be a novel pathway for HSPC migration anteriorly to colonize the developing

kidney marrow, the adult definitive hematopoietic organ in zebrafish. Although time-lapse analyses showed that the PD-located HSPCs are derived from the dorsal AGM, where the definitive HSCs originally develop, other sites contributing to the PD-HSPCs are possible. Indeed, an increased number of *scl*$^{+}$ HSPCs detected in the PD of C/ebpαDN embryos raises the possibility of both PBI-derived EMPs and ICM-derived HSPCs as another source of PD-HSPCs. In addition, we also detected a specific up-regulation of CD41, a marker for PBI-derived EMPs, but not for ICM-derived HSPCs by C/ebpαDN at 22 hpf (supplemental Figure 14), suggesting that the PBI-derived EMPs are probably the major cell source of PD-HSPCs and cause of erythropoietic dysplasia.

In conclusion, it should be pointed out that a unique characteristic in the current study is the use of the *lmo2* promoter to drive the expression of C/ebpαDN and Bmi1. The *lmo2* promoter activity is transient, peaking at 22 hpf and hardly detected by WISH and Western blot analyses after 24 hpf, which results in the rapid wane of primitive hematopoietic wave. This feature provides a unique opportunity to investigate the fate and consequence of the short-lived HSPCs once reprogrammed by "pulsed" or instantaneous expression of either C/ebpαDN or Bmi1. However, a potential disadvantage of using the *lmo2* promoter is that the progeny of these reprogrammed HSPCs in the CHT region ~ 75 hpf can no longer be followed up by EGFP fluorescence because of the lack of the sustained expression of EGFP-tagged proteins. Replacing the *lmo2* promoter with a ubiquitously and sustainably activated promoter such as β-actin promoter, in combination with the *Tg(lmo2:Cre)* transgenic line, should complement the technical limitation.

Acknowledgments

The authors thank the anonymous reviewer I for insightful comments, and Dr Li-Ping Su and all the members of our laboratory for helpful discussions.

This work was supported in part by the National Basic Research Program of China (2007CB947003 and 2011CB964803), the National Natural Science Foundation of China (30525019, 30830047), Science and Technology Commission of Shanghai Municipality (09XD1404700), and the Strategic Priority Research Program of the Chinese Academy of Science (XDA 01010106).

Authorship

Contribution: T.Z., L.W., and K.-Y.Z. performed experiments and analyzed data; M. Dong, P.-F.X., Y.C., and M. Deng assisted with experiments; M. Deng, S.-J.C., Z.C., and T.X.L. designed the research plan; and T.Z. and T.X.L. wrote the paper.

Conflict-of-interest disclosure: The authors declare no competing financial interests.

Correspondence: Ting Xi Liu, Laboratory of Development and Diseases, Institute of Health Sciences, Room 408, Building 1, 225 South Chong Qing Road, Shanghai, People's Republic of China 200025; e-mail: txliu@sibs.ac.cn.

References

1. Godin I, Cumano A. The hare and the tortoise: an embryonic haematopoietic race. *Nat Rev Immunol.* 2002;2(8):593-604.
2. Chen AT, Zon LI. Zebrafish blood stem cells. *J Cell Biochem.* 2009;108(1):35-42.
3. Lieschke GJ, Oates AC, Paw BH, et al. Zebrafish SPI-1 (PU.1) marks a site of myeloid development independent of primitive erythropoiesis: implications for axial patterning. *Dev Biol.* 2002; 246(2):274-295.
4. Shepard JL, Zon LI. Developmental derivation of embryonic and adult macrophages. *Curr Opin Hematol.* 2000;7(1):3-8.
5. Herbomel P, Thisse B, Thisse C. Ontogeny and behaviour of early macrophages in the zebrafish embryo. *Development.* 1999;126(17):3735-3745.
6. Le Guyader D, Redd MJ, Colucci-Guyon E, et al. Origins and unconventional behavior of neutrophils in developing zebrafish. *Blood.* 2008;111(1): 132-141.
7. Liu TX, Rhodes J, Deng M, et al. Dominant-interfering C/EBPalpha stimulates primitive erythropoiesis in zebrafish. *Exp Hematol.* 2007;35(2): 230-239.
8. Rhodes J, Hagen A, Hsu K, et al. Interplay of pu.1 and gata1 determines myelo-erythroid progenitor cell fate in zebrafish. *Dev Cell.* 2005;8(1):97-108.
9. Warga RM, Kane DA, Ho RK. Fate mapping embryonic blood in zebrafish: multi- and unipotential lineages are segregated at gastrulation. *Dev Cell.* 2009;16(5):744-755.
10. Bennett CM, Kanki JP, Rhodes J, et al. Myelopoiesis in the zebrafish, Danio rerio. *Blood.* 2001; 98(3):643-651.
11. Bertrand JY, Kim AD, Violette EP, Stachura DL, Cisson JL, Traver D. Definitive hematopoiesis initiates through a committed erythromyeloid progenitor in the zebrafish embryo. *Development.* 2007;134(23):4147-4156.
12. Cumano A, Godin I. Ontogeny of the hematopoietic system. *Annu Rev Immunol.* 2007;25:745-785.
13. Murayama E, Kissa K, Zapata A, et al. Tracing hematopoietic precursor migration to successive hematopoietic organs during zebrafish development. *Immunity.* 2006;25(6):963-975.
14. Kissa K, Murayama E, Zapata A, et al. Live imaging of emerging hematopoietic stem cells and early thymus colonization. *Blood.* 2008;111(3): 1147-1156.
15. Bertrand JY, Kim AD, Teng S, Traver D. CD41+ cmyb+ precursors colonize the zebrafish pronephros by a novel migration route to initiate adult hematopoiesis. *Development.* 2008;135(10): 1853-1862.
16. Zhang P, Iwasaki-Arai J, Iwasaki H, et al. Enhancement of hematopoietic stem cell repopulating capacity and self-renewal in the absence of the transcription factor C/EBP alpha. *Immunity.* 2004;21(6):853-863.
17. Zhang DE, Zhang P, Wang ND, Hetherington CJ, Darlington GJ, Tenen DG. Absence of granulocyte colony-stimulating factor signaling and neutrophil development in CCAAT enhancer binding protein alpha-deficient mice. *Proc Natl Acad Sci U S A.* 1997;94(2):569-574.
18. Pabst T, Mueller BU, Zhang P, et al. Dominant-negative mutations of CEBPA, encoding CCAAT/enhancer binding protein-alpha (C/EBPalpha), in acute myeloid leukemia. *Nat Genet.* 2001;27(3): 263-270.
19. Nerlov C. C/EBPalpha mutations in acute myeloid leukaemias. *Nat Rev Cancer.* 2004;4(5):394-400.
20. Wang C, Chen X, Wang Y, Gong J, Hu G. C/EBPalphap30 plays transcriptional regulatory roles distinct from C/EBPalphap42. *Cell Res.* 2007; 17(4):374-383.
21. Fu CT, Zhu KY, Mi JQ, et al. An evolutionarily conserved PTEN-C/EBPalpha-CTNNA1 axis controls myeloid development and transformation. *Blood.* 2010;115(23):4715-4724.
22. Lessard J, Sauvageau G. Bmi-1 determines the proliferative capacity of normal and leukaemic stem cells. *Nature.* 2003;423(6937):255-260.
23. Park IK, Qian D, Kiel M, et al. Bmi-1 is required for maintenance of adult self-renewing haematopoietic stem cells. *Nature.* 2003;423(6937):302-305.
24. Chowdhury M, Mihara K, Yasunaga S, Ohtaki M, Takihara Y, Kimura A. Expression of Polycomb-group (PcG) protein BMI-1 predicts prognosis in patients with acute myeloid leukemia. *Leukemia.* 2007;21(5):1116-1122.
25. Leung C, Lingbeek M, Shakhova O, et al. Bmi1 is essential for cerebellar development and is overexpressed in human medulloblastomas. *Nature.* 2004;428(6980):337-341.
26. Kimmel CB, Ballard WW, Kimmel SR, Ullmann B, Schilling TF. Stages of embryonic development of the zebrafish. *Dev Dyn.* 1995;203(3):253-310.
27. Wang L, Zhang Y, Zhou T, et al. Functional characterization of Lmo2-Cre transgenic zebrafish. *Dev Dyn.* 2008;237(8):2139-2146.
28. Zhu H, Traver D, Davidson AJ, et al. Regulation of the lmo2 promoter during hematopoietic and vascular development in zebrafish. *Dev Biol.* 2005;281(2):256-269.
29. Thermes V, Grabher C, Ristoratore F, et al. I-SceI meganuclease mediates highly efficient transgenesis in fish. *Mech Dev.* 2002;118(1):91-98.
30. Link V, Shevchenko A, Heisenberg CP. Proteomics of early zebrafish embryos. *BMC Dev Biol.* 2006;6:1.
31. Yeh JR, Munson KM, Chao YL, Peterson QP, Macrae CA, Peterson RT. AML1-ETO reprograms hematopoietic cell fate by downregulating scl expression. *Development.* 2008;135(2):401-410.
32. Sun XJ, Xu PF, Zhou T, et al. Genome-wide survey and developmental expression mapping of zebrafish SET domain-containing genes. *PLoS One.* 2008;3(1):e1499.

33. Fu YF, Du TT, Dong M, et al. Mir-144 selectively regulates embryonic alpha-hemoglobin synthesis during primitive erythropoiesis. *Blood.* 2009; 113(6):1340-1349.

34. Zhang Y, Bai XT, Zhu KY, et al. In vivo interstitial migration of primitive macrophages mediated by JNK-matrix metalloproteinase 13 signaling in response to acute injury. *J Immunol.* 2008;181(3): 2155-2164.

35. Jin H, Sood R, Xu J, et al. Definitive hematopoietic stem/progenitor cells manifest distinct differentiation output in the zebrafish VDA and PBI. *Development.* 2009;136(4):647-654.

36. Liao EC, Paw BH, Oates AC, Pratt SJ, Postlethwait JH, Zon LI. SCL/Tal-1 transcription factor acts downstream of cloche to specify hematopoietic and vascular progenitors in zebrafish. *Genes Dev.* 1998;12(5):621-626.

37. Goyama S, Yamamoto G, Shimabe M, et al. Evi-1 is a critical regulator for hematopoietic stem cells and transformed leukemic cells. *Cell Stem Cell.* 2008;3(2):207-220.

38. Mochizuki N, Shimizu S, Nagasawa T, et al. A novel gene, MEL1, mapped to 1p36.3 is highly homologous to the MDS1/EVI1 gene and is transcriptionally activated in t(1;3)(p36;q21)-positive leukemia cells. *Blood.* 2000;96(9): 3209-3214.

39. Zon LI. Intrinsic and extrinsic control of haematopoietic stem-cell self-renewal. *Nature.* 2008; 453(7193):306-313.

40. Bhardwaj G, Murdoch B, Wu D, et al. Sonic hedgehog induces the proliferation of primitive human hematopoietic cells via BMP regulation. *Nat Immunol.* 2001;2(2):172-180.

41. Iwama A, Oguro H, Negishi M, et al. Enhanced self-renewal of hematopoietic stem cells mediated by the polycomb gene product Bmi-1. *Immunity.* 2004;21(6):843-851.

42. Iwama A, Oguro H, Negishi M, Kato Y, Nakauchia H. Epigenetic regulation of hematopoietic stem cell self-renewal by polycomb group genes. *Int J Hematol.* 2005;81(4):294-300.

43. Ohta H, Sawada A, Kim JY, et al. Polycomb group gene rae28 is required for sustaining activity of hematopoietic stem cells. *J Exp Med.* 2002; 195(6):759-770.

44. Suh HC, Gooya J, Renn K, Friedman AD, Johnson PF, Keller JR. C/EBPalpha determines hematopoietic cell fate in multipotential progenitor cells by inhibiting erythroid differentiation and inducing myeloid differentiation. *Blood.* 2006; 107(11):4308-4316.

45. Wagner K, Zhang P, Rosenbauer F, et al. Absence of the transcription factor CCAAT enhancer binding protein alpha results in loss of myeloid identity in bcr/abl-induced malignancy. *Proc Natl Acad Sci U S A.* 2006;103(16):6338-6343.

46. Alkema MJ, Wiegant J, Raap AK, Berns A, van Lohuizen M. Characterization and chromosomal localization of the human proto-oncogene BMI-1. *Hum Mol Genet.* 1993;2(10):1597-1603.